Reverse-time (and Kirchhoff) migration

Rodrigue Lelotte & Jules Sanchez

1. Preliminaries.

We consider the two-dimensional euclidian space as the medium, purported to be homogeneous ($c(x) \equiv 1$). Let us derive an analytical formula for the time-harmonic Green's function $\widehat{G}_0(\omega,x,y)$, that is the Fourier transform of the Green's function $G_0(t,x,y)$ w.r.t. the time variable t, which we recall to satisfy the *Helmholtz equation*, *i.e.*

$$\Delta_x \widehat{G}_0(\omega,x,y) + \omega^2 \widehat{G}_0(\omega,x,y) = -\delta(x-y). \tag{1.1}$$

By taking the Fourier transform $\mathscr{F}_x$ w.r.t. the space variable x of (1.1), we obtain

$$-|k_x|^2 \mathscr{F}_x \widehat{G}_0(\omega,k,y) + \omega^2 \mathscr{F}_x \widehat{G}_0(\omega,k,y) = -\exp(ik\cdot y)/(2\pi). \tag{1.2}$$

from which it follows that $\mathscr{F}_x \widehat{G}_0(\omega,k,y) = -\exp(ik\cdot y)/(2\pi[\omega^2 - |k|^2])$. Therefore, one has

$$\widehat{G}_0(\omega,x,y) = \mathscr{F}_x^{-1}[\mathscr{F}_x \widehat{G}_0](\omega,x,y) = \frac{1}{(2\pi)^2}\int_{\mathbb{R}^2} \frac{\exp(ik\cdot(x-y))}{|k_x|^2 - \omega^2}\mathrm{d}k. \tag{1.3}$$

Remark 1.1. *Given a function $\mathbb{R} \ni r \mapsto f(r)$, one defines the* ν-th Hankel transform *of f as*

$$\mathscr{H}_\nu[f](k) := \int_0^\infty f(r) J_\nu(kr) r dr,$$

where J_ν is the ν-th Bessel function of the first kind*, that is*

$$J_\nu(z) = \frac{(-i)^n}{2\pi}\int_0^{2\pi} \exp(iz\cos(\varphi) + in\varphi) d\varphi.$$

The ν-th Hankel transform expresses any given function f as a weighted-sum of an infinite number of rescaled *Bessel functions of the first kind J_ν. That is, in comparison with the Fourier transform, the dual variable is no longer the* frequency *as it is some* scaling factor.

Wisely rotating the frame of coordinates and carrying the computations into the polar domain yields that

$$\widehat{G}_0(\omega,x,y) = \frac{1}{(2\pi)^2}\int_0^\infty \frac{r\mathrm{d}r}{r^2-\omega^2}\left[\int_0^{2\pi}\exp\left(ir\cos(\varphi)|x-y|\right)\mathrm{d}\varphi\right] = \frac{1}{2\pi}\mathscr{H}_0\left[\frac{1}{r^2-\omega^2}\right](|x-y|).$$

It remains to compute the 0-th Hankel transform of $f : r \mapsto 1/(r^2-\omega^2)$. The neat trick here is to write

$$\mathscr{H}_0[f](k) = \int_0^\infty \mathscr{L}^{-1}[rf(r)](s)\mathscr{L}[J_0(kr)](s)\mathrm{d}s,$$

where $\mathscr{L}$ (resp. $\mathscr{L}^{-1}$) denotes the (resp. inverse) Laplace transform, and we have

$$\mathscr{L}[J_0(kr)](s) = \frac{1}{\sqrt{k^2+s^2}}, \qquad \mathscr{L}^{-1}[rf(r)] = \cos(-i\omega s),$$

so that we obtain (after change of variable $s \to s/|x-y|$)

$$\widehat{G}_0(\omega,x,y) = \frac{1}{2\pi}\int_0^\infty \frac{\cos(-i|x-y|\omega s)}{\sqrt{s^2+1}}\mathrm{d}s = \frac{1}{2\pi}K_0(-i|x-y|\omega) = \frac{i}{4}H_0(\omega|x-y|),$$

with K_0 the 0-*th modified Bessel function of the second kind*, and H_0 the 0-*th Hankel function*, where the last two equalities are common knowledge in the field of special functions. A more pedestrian derivation, not resorting to Hankel transform, is possible by using contour integrals.

2. Time-harmonic localization – full aperture.

2.1. Theoretical background

The embedded reflector x_{ref} is modeled by a local variation $V(x)$ of the propagation speed $c(x)$ in the vicinity of the reflector, where we suppose that $V(x) = \sigma_{\mathrm{ref}} \cdot \mathbb{1}_{\Omega_{\mathrm{ref}}}(x-x_{\mathrm{ref}})$ where σ_{ref} is the target reflectivity and Ω_{ref} is the small scattering region of area ℓ_{ref}^2 which corresponds to the reflector apparatus. We assume that ℓ_{ref} is negligible w.r.t. the typical wavelength $\lambda = 2\pi/\omega$, such that we can suppose that $V(x) \simeq \sigma_{\mathrm{ref}}\ell_{\mathrm{ref}}^2 \cdot \delta(x-x_{\mathrm{ref}})$. Using Born approximation, the Green's function reads

$$\widehat{G}_{\mathrm{ref}}(\omega,x,y) = \widehat{G}_0(\omega,x,y) + \omega^2\sigma_{\mathrm{ref}}\ell_{\mathrm{ref}}^2 \cdot \widehat{G}_0(\omega,x,x_{\mathrm{ref}})\widehat{G}_0(\omega,x_{\mathrm{ref}},y).$$

We record the impulse response matrix $(\widehat{u}_{rs}(\omega))_{r,s}$, where $\widehat{u}_{rs}(\omega)$ is the time-harmonic amplitude recorded by the r-th receiver when the s-th source emits a time-harmonic signal with unit amplitude and frequency ω. Equalizing the data, that is removing the incident field (*i.e.* not scattered), we have that

$$\widehat{u}_{rs}(\omega) = \omega^2\sigma_{\mathrm{ref}}\ell_{\mathrm{ref}}^2 \cdot \widehat{G}_0(\omega,x_r,x_{\mathrm{ref}})\widehat{G}_0(\omega,x_{\mathrm{ref}},x_s), \quad \forall r,s. \tag{2.1}$$

2.1.1. *Reverse-time imaging*

Recall that the Reverse-time (RT) imaging function for the search point x^S is defined as

$$\mathscr{I}_{\mathrm{RT}}(\omega, x^S) := \frac{1}{N^2} \sum_{r,s} \widehat{G}_0(\omega, x^S, x_r) \widehat{G}_0(\omega, x_s, x^S) \overline{\widehat{u}_{rs}(\omega)} \tag{2.2}$$

If the number of transducers is high enough, *i.e.* $N \gg 1$, we can assume that we have a continuum of transducers on $\partial B(0, R_0)$, so that plugging the impulse responses (2.1) into (2.2) yields the approximation (using *reciprocity* of the time-harmonic Green's function)

$$\mathscr{I}_{\mathrm{RT}}(\omega, x^S) \simeq \omega^2 \sigma_{\mathrm{ref}} \ell_{\mathrm{ref}}^2 \cdot \left[\int_{x \in \partial B(0,R_0)} \widehat{G}_0(\omega, x^S, x) \overline{\widehat{G}_0(\omega, x_{\mathrm{ref}}, x)} \mathrm{d}\sigma(x) \right]^2 .$$

Moreover, if $R_0 \gg 1$, we can invoke *Helmholtz-Kirchhoff identity*, so that we eventually have that the theoretical focal spot is given by

$$\mathscr{I}_{\mathrm{RT}}(\omega, x^S) \simeq \sigma_{\mathrm{ref}} \ell_{\mathrm{ref}}^2 \cdot \Im \widehat{G}_0(\omega, x^S, x_{\mathrm{ref}})^2 = \sigma_0 \cdot J_0^2(\omega |x^S - x_{\mathrm{ref}}|)$$

with $\sigma_0 := \sigma_{\mathrm{ref}} \ell_{\mathrm{ref}}^2 / 16$.

2.1.2. *Kirchhoff migration imaging*

Let us now see how to extend the Kirchhoff migration (KM) imaging to the two-dimensional setting. For large $|z|$, we have the following simple asymptotic $H_0(z) \sim \sqrt{\frac{2}{\pi z}} \cdot e^{i(z - \pi/4)}$, so that if we neglect the variations of the amplitude term in the time-harmonic Green's function $\widehat{G}_0$, one has

$$\mathscr{I}_{\mathrm{RT}}(\omega, x^S) \simeq \frac{1}{N^2} \sum_{r,s} e^{i\omega(|x^S - x_r| - |x_{\mathrm{ref}} - x_r|)} e^{i\omega(|x^S - x_s| - |x_{\mathrm{ref}} - x_s|)} = \left[\frac{1}{N} \sum_{r} e^{i\omega(|x^S - x_r| - |x_{\mathrm{ref}} - x_r|)} \right]^2 .$$

Once again, if $N \gg 1$, we can assume that we have a continuum of transducers on $\partial B(0, R_0)$, so that

$$\mathscr{I}_{\mathrm{RT}}(\omega, x^S) \simeq \left(\int_{x \in \partial B(0,R_0)} \exp\Big[i\omega(|x^S - x| - |x_{\mathrm{ref}} - x|) \Big] \mathrm{d}\sigma(x) \right)^2 .$$

If $R_0 \gg \max\{|x^S|, |x_{\mathrm{ref}}|\}$, we get from simple geometrical arguments that

$$|x^S - x| - |x_{\mathrm{ref}} - x| \simeq \langle x_{\mathrm{ref}} - x^S, R_0^{-1} x \rangle$$

for every $x \in \partial B(0,R_0)$. Carrying the computations of the contour integral into the polar domain, *i.e.* $x = (R_0\cos(\theta), R_0\sin(\theta))$, and using the fact that there exists $\phi_{S,\mathrm{ref}} \in [0,2\pi)$ such that

$$\langle x_{\mathrm{ref}} - x^S, R_0^{-1}x\rangle = |x^S - x_{\mathrm{ref}}|\cos(\theta + \phi_{S,\mathrm{ref}}), \quad \forall\theta,$$

we have

$$\int_{x\in\partial B(0,R_0)} \ldots \mathrm{d}\sigma(x) \simeq \int_0^{2\pi} \exp\Big[i\omega|x^S - x_{\mathrm{ref}}|\cos(\theta+\phi_{S,\mathrm{ref}})\Big]\mathrm{d}\theta,$$

so that we recognize the 0-*th modified Bessel function* I_0 *of the first kind*, which we recall to have the integral representation $(2\pi)I_0(z) = \int_0^{2\pi} e^{z\cos(\theta)}\mathrm{d}\theta$, therefore yielding we can take the *theoretical* Kirchhoff migration imaging function at the search point x^S to be

$$\mathscr{I}_{\mathrm{KM}}^{(th)}(\omega, x^S) := I_0^2(i\omega|x^S - x_{\mathrm{ref}}|).$$

In practice, we don't have access to x_{ref}, since we are precisely looking for this quantity. Therefore, a possible rough ansatz would be to simply define

$$\mathscr{I}_{\mathrm{KM}}^{(an)}(\omega, x^S) := \frac{1}{N^2}\sum_{r,s} e^{i\omega(|x^S - x_s| + |x^S - x_r|)}\overline{\widehat{u}_{rs}(\omega)}.$$

2.2. Numerical experiments

Default parameters – We conduct a first numerical experiment with $N = 100$ transducers evenly-disposed on a circular array of radius $R_0 = 100$ centered at the origin. The reflector is positioned at locus $x_{\mathrm{ref}} = (10,20)$, and the source signals are taken to be time-harmonic wave of frequency $\omega = 2\pi$. The resolution of the discretization grid for the search space is taken to 20×20 centered at x_{ref}. Color-maps of the module of the time-reversal refocusing imaging functions obtained through RT and KM heuristics are displayed on fig. 1. We notice that KM and RT performances are very similar to one another, and that both techniques produce imaging functionals that are very close to the theoretical focal spot as derived above.

Moving the reflector – Getting the reflector closer to the boundary inherently deteriorates the resolution of the time-reverse refocusing. One possible way to overcome this problem is to increase the frequency ω of the search beam. Indeed, in the case where $\lambda \gg d(x_{\mathrm{ref}}, \partial B(0,R_0))$ where $\lambda = 2\pi/\omega$, because the typical wavelength of the source beams is much larger than the distance between the near-located transducers and the reflector, we expect that those transducers that are close to x_{ref} will contaminate the overall refocusing process. This intuition is largely confirmed by our numerical experiment, see figs. 2 to 4. From those experiments, it pertains that KM imaging seems to perform slightly better that RT when the reflector is closed to the transducers array. This might be explained

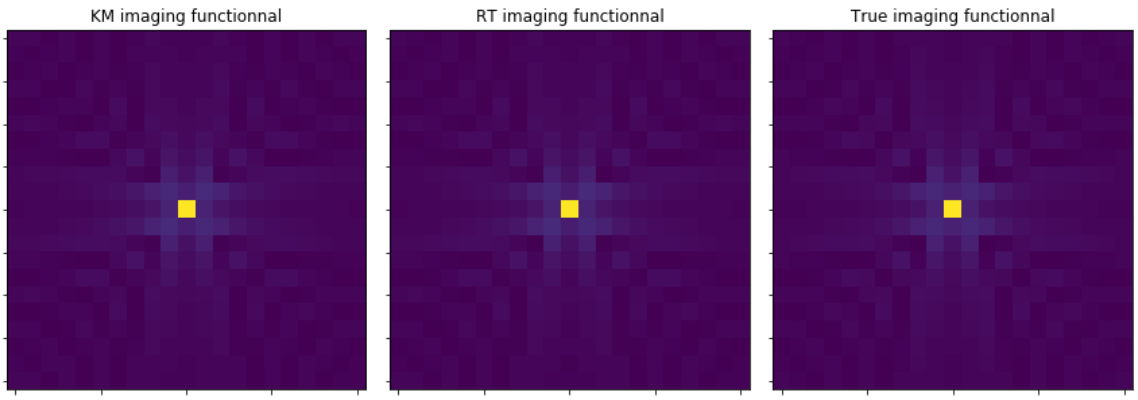

Fig. 1: Comparison of KM imaging (left) with RT imaging (center), and the theoretical focal spot (right). The search area in centered around $x_{\text{ref}} = (10, 20)$, with parameters $\omega = 2\pi$, $N = 100$ and $R_0 = 100$.

by the inherent singularities of the time-harmonic Green's function $\widehat{G}_0(\omega, \cdot, \cdot)$ on its diagonal (*i.e.* $Y_0(x) \to -\infty$ as $x \to 0^+$). It is also important to notice that increasing the frequency translates into a higher demand for physical energy, which might come very costly.

Changing the number of transducers – Decreasing the number N of transducers also deteriorates the resolution, as confirmed by numerical experiments, see fig. 5 below. This is trivially fathomed: less transducers means that less information goes into the system, so that it is much harder to refocus in one pass. Note that this might be overcame by iterating the previous process several times, allowing for a better refocusing resolution at each pass.

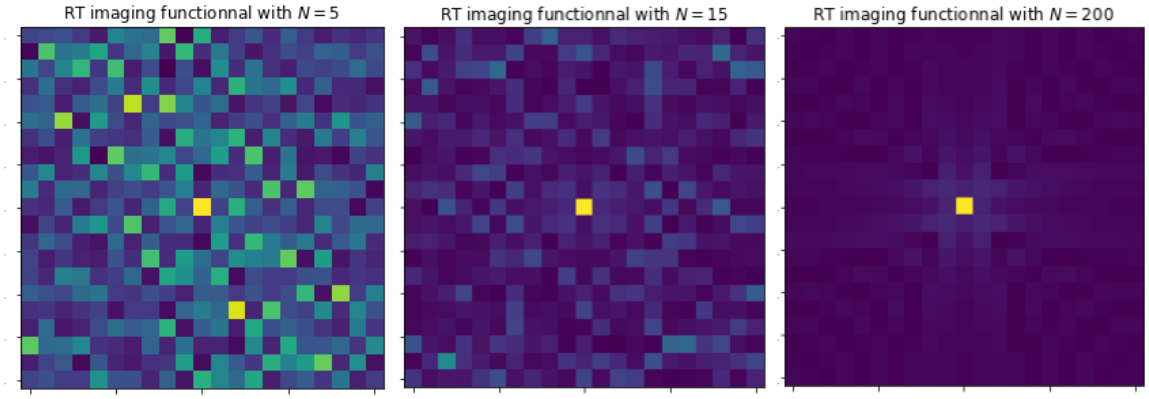

Fig. 5: Comparison of RT imaging with $N = 5$ transducers (left), $N = 15$ (center) and $N = 200$ (right). As expected, the resolution greatly deteriorates as N decreases. This applies to KM imaging as well.

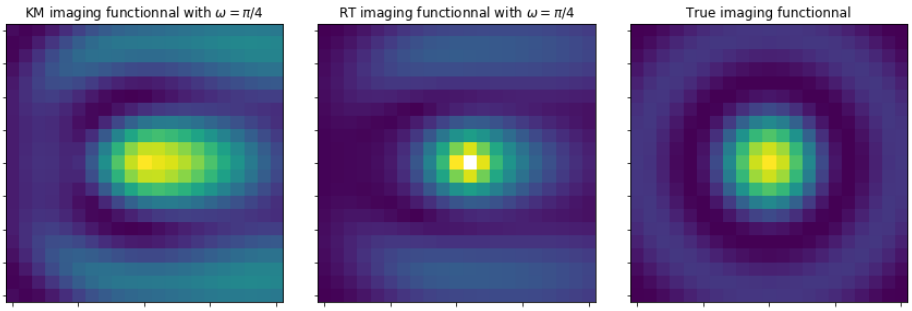

Fig. 2: Comparison of KM imaging (left) and RT imaging (center) with the theoretical spot (right) when the reflectors is positioned at locus $x_{\text{ref}} = (99.5, 0)$ and $\omega = \pi/4$ (all other parameters are left unchanged). White spot on the RT imaging corresponds to the closest transducer.

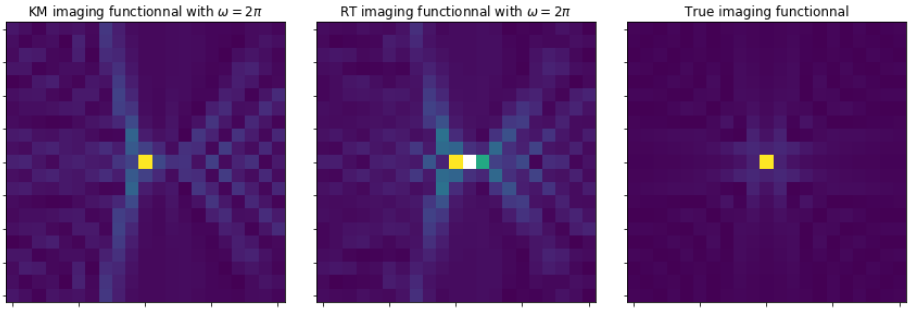

Fig. 3: Same comparison as above, but this time with the default frequency parameter $\omega = 2\pi$. Resolution is improved compared to the previous case, as expected from a physical point-of-view. Notice that KM performs slightly better that RT.

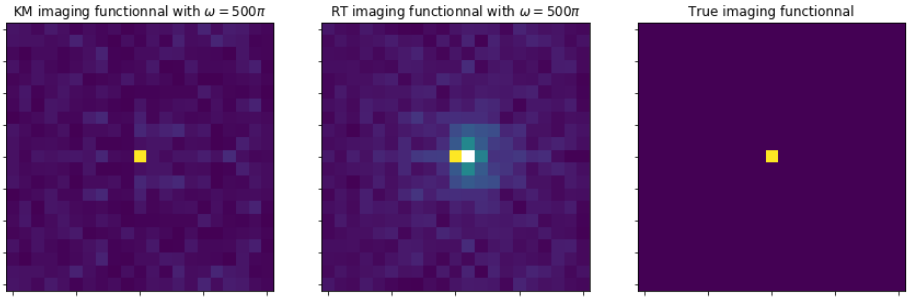

Fig. 4: Same comparison as above, but this time with very-high frequency $\omega = 500\pi$. Resolution is greatly improved in the search area compared to the previous cases, and we recover similar imaging functions as when the reflector was buried far away from the circular transducers array. Notice that KM performs with far more precision than RT.

3. Time-harmonic localization – partial aperture.

Let us give an *rough approximate* proof for the exact focal spot formula in the cross-range direction (x-direction) in the partial-aperture setting. First, we assume that we have a continuum of uniformly distributed transducers on $[-R_0/2, R_0/2]$. If the height L of the reflector x_{ref} (*i.e.* $x_{\text{ref}} = (0, L)$) is high enough, so that we can use Hankel's function expansion as before and neglect the variations of the amplitude term, we have the approximation

$$\mathscr{I}_{RT}(\omega, (x^S, 0)) \simeq \omega^2 \sigma_{\text{ref}} \ell_{\text{ref}}^2 \cdot \left[\int \mathbb{1}_{[-R_0/2, R_0/2]}(x_r) e^{i\omega(|x_{\text{ref}} - (x_r, 0)| - |x^S - x_r|)} \mathrm{d}x_r \right]^2.$$

Under the regime where $L \gg R_0$, we have that

$$\begin{aligned} |x_{\text{ref}} - (x_r, 0)| - |x^S - x_r| &\simeq \left\langle (x^S, 0) - x_{\text{ref}}, \frac{(x_r, 0) - x_{\text{ref}}}{|(x_r, 0) - x_{\text{ref}}|} \right\rangle \\ &= |(x^S, 0) - x_{\text{ref}}| \cdot \underbrace{\text{Angle}\left((x^S, 0) - x_{\text{ref}}, (x_r, 0) - x_{\text{ref}} \right)}_{\simeq (x^S - x_r)/L}. \end{aligned}$$

Therefore, getting rid of the phase term, we obtain that

$$\begin{aligned} \mathscr{I}_{RT}(\omega, (x^S, 0)) &\simeq \omega^2 \sigma_{\text{ref}} \ell_{\text{ref}}^2 \cdot \left[\int \mathbb{1}_{[-R_0/2, R_0/2]}(x_r) e^{-i\omega x_r \frac{|(x^S, 0) - x_r|}{L}} \mathrm{d}x_r \right]^2 \\ &= (2\pi)^2 \omega^2 \sigma_{\text{ref}} \ell_{\text{ref}}^2 \cdot \left[\widehat{\mathbb{1}}_{[-R_0/2, R_0/2]} \left(\frac{|(x^S, 0) - x_r|}{L} \right) \right]^2, \end{aligned}$$

and using the well-known fact that $\widehat{\mathbb{1}}_{[-R_0/2, R_0/2]}(\xi) = (\pi R_0/2) \cdot \text{sinc}(\xi R_0/2)$, we roughly find the mentioned result. Note that the oscillating behavior as $|x^S| \to \infty$ is coherent with the phenomenon of *edge diffraction*.

4. Time-dependent localization – partial aperture.

We now assume that the sources emit a broadband signal f with $\widehat{f}(\omega) = \mathbb{1}_{[\omega_0 - B, \omega_0 + B]}(\omega)$. In this context, the Reverse-time imaging function at the search point x^S reads

$$\mathscr{I}_{RT}(\omega_0, B, x^S) = \frac{1}{N^2} \int_{\omega_0 - B}^{\omega_0 + B} \sum_{r,s} \widehat{G}_0(\omega, x^S, x_r) \widehat{G}_0(\omega, x_s, x^S) \overline{\widehat{u}_{rs}(\omega)} \mathrm{d}\omega$$

5. Stability with respect to measurement noise.

We add measurement noises to our previous settings, that is, we consider that the recorded signals are of the form $\widehat{u}_{rs}(\omega) + W_{rs}^{(1)}(\omega) + iW_{rs}^{(2)}(\omega)$, where $W_{rs}^{(1)}(\omega)$ and $W_{rs}^{(2)}(\omega)$ are i.i.d. Gaussian random variables with mean zero and variance $\sigma^2/2$. Let us write $\mathscr{I}_0(\omega, x^S)$ for the unperturbated imaging function (2.2), such that the Reverse-time imaging function at the search point x^S reads

$$\mathscr{I}_{RT}(\omega, x^S) = \mathscr{I}_0(\omega, x^S) + \mathscr{I}_{\text{noise}}(\omega, x^S),$$

where $\mathscr{I}_{\text{noise}}(\omega, x^S)$ is the complex Gaussian random field generated by the $W_{rs}^{(1/2)}$'s.